

# Prospect of measuring the top quark mass through energy correlators

---

**Meng Xiao, Yulei Ye, and Xinyu Zhu**

*School of Physics, Zhejiang University, Hangzhou, Zhejiang 310058, China*

*E-mail:* [mxiao@zju.edu.cn](mailto:mxiao@zju.edu.cn), [ylye@zju.edu.cn](mailto:ylye@zju.edu.cn), [xy\\_zhu@zju.edu.cn](mailto:xy_zhu@zju.edu.cn)

**ABSTRACT:** Reaching a high precision of the top quark mass is an important task of the Large Hadron Collider. We perform a feasibility study of measuring the top quark mass through the three-point energy correlator. The expected sensitivity of the top quark mass in the boosted regime is presented. We further introduce its application to the low top  $p_T$  regime and demonstrate that both the W boson and the top quark masses could be extracted from this single observable. Compared to traditional observables, the energy correlator shows robustness to uncertainties that usually dominate experimental measurements and provides a promising way to improve experimental precision.

## 1 Introduction

The top quark is the heaviest elementary particle in the Standard Model. The precision of its mass, together with that of the Higgs boson, plays a central role in determining the stability of the electroweak vacuum [1–4]. While the precise measurement of the top quark mass has been one of the most important campaigns at the Large Hadron Collider (LHC), the yielded uncertainty is the largest among those of the heavy elementary particles [5].

Various strategies have been developed to precisely measure the top quark mass  $m_t$  [6–19], among which the most precise one comes from the direct measurements [10], where the top quark is treated as a free particle and Monte-Carlo (MC) based simulation is used to extract the  $m_t$ . The experimental signature and the corresponding measurement vary with the transverse momentum of the top quark  $p_T^{\text{top}}$ . The low  $p_T^{\text{top}}$  region, often called the resolved regime, presents a final state with three particles decayed from the top quark and well-separated from each other. Experiments usually reconstructed the invariant masses from the three objects to measure the  $m_t$ . As the  $p_T^{\text{top}}$  increases, the decayed products get Lorentz-boosted, making the hadronic decay products of the top quark non-resolvable and forming a single large jet. Typical observables for the  $m_t$  measurement in this regime are the invariant jet mass.

For both  $p_T^{\text{top}}$  regimes, the reconstructed invariant masses are subject to uncertainties in the jet  $p_T$ , such as the jet energy scale uncertainty (JES). Although the JES has been constrained experimentally by the precisely known W boson mass [10, 19], it still dominates the uncertainties in these measurements. Recently, energy correlators inside jets have been proposed to study the properties of heavy particles such as the top quark mass [20, 21] in the boosted regime. They have the advantage of being theoretically calculable and, therefore could be used to extract the pole mass of the top quark. These correlators have been measured for light flavor jets by the CMS collaboration [22], demonstrating that high-precision measurements of the observable could be reached.

In this paper, we illustrate that the energy correlator is an ideal observable to reduce the impact of JES in top mass measurements. It is powerful to improve the precision of the  $m_t$  not only in the boosted regime but also in the resolved regime. We first present its sensitivity to the  $m_t$  in the boosted region using MC simulations, where the projected three-point energy correlator (E3C) is compared with the jet invariant mass  $m_{\text{jet}}$ , and better resilience to systematic uncertainties such as JES is observed. We then extend the method to the low  $p_T^{\text{top}}$  regions, where two peaks resulting from the W boson and the top quark could be observed simultaneously in the E3C distribution. The intriguing features of the peaks make the E3C a promising observable to improve the  $m_t$  precision in the resolved region.

## 2 E3C and its application to top quark

Multi-point energy correlators [23–25] are a class of observables that describe the energy-weighted angular correlations between particles. Specifically, the E3C focuses on the correlation among three particles. The theoretical definition of E3C is [26, 27]

$$\text{E3C} = \frac{d\sigma}{dx_L} = \sum_{i,j,k}^n \int d\sigma \frac{E_i E_j E_k}{E^3} \delta(x_L - \max(\Delta R_{ij}, \Delta R_{ik}, \Delta R_{jk})). \quad (2.1)$$

At hadron colliders, they are proposed for jet substructure studies. In its application to boosted top jets [20], the particle indices  $i, j, k$  run overall all the  $n$  particles in a top jet, and  $E$  is the summed energy of all the particles, equivalent to the jet energy. The largest  $\Delta R_{ij} = \sqrt{\Delta\eta^2 + \Delta\phi^2}$  of the triangle formed by  $i, j, k$  particles is denoted by  $x_L$ . Since the top quark decays to three particles, E3C is a natural probe for the top decay. The distribution of E3C is a function of  $x_L$  with energy weight  $E_i E_j E_k / E^3$ . Experimental resolution of angles is much better than the energies, therefore compared to invariant mass type observables, E3C could be measured with higher precision. In addition, the weight makes the observable robust to uncertainties that systematically change the energy of the jet constituents, since the changes largely cancel in the ratio.

### 3 Top mass sensitivity in the boosted region

We start by examining the sensitivity of the E3C observable to the  $m_t$  in the boosted top region. MC simulation of the  $t\bar{t}$  semi-leptonic process is used. According to experimental measurements [28], this process yields the highest sensitivity. The events are generated with MADGRAPH5\_aMC@NLO [29, 30] at leading-order (LO) of QCD and interfaced to PYTHIA8 [31] for parton shower and hadronization. Multiple samples are generated with different top quark masses, ranging from 168 GeV to 174 GeV. The mass of the W boson is set to 80.4 GeV. To select the hadronically decayed top quark, anti- $k_T$  algorithm [32] is performed by FastJet [33, 34] with parameter  $R = 1.2$ . An event is required to have at least two jets with  $p_T^{\text{top}} > 400$  GeV and  $|\eta| < 2.4$  and a lepton with  $p_T > 60$  GeV and  $|\eta| < 2.4$ . The leading jet is required to be further away from the lepton compared to the sub-leading jet, and it is used to evaluate the sensitivity to the  $m_t$ .

Here we compare the performances of E3C to  $m_{\text{jet}}$ . CMS has used  $m_{\text{jet}}$  to measure the  $m_t$  with a relative uncertainty of 1.45% [11] with  $36 \text{ fb}^{-1}$  data and the uncertainty was further reduced to 0.50% [19] after constraining JES uncertainty using the W mass with  $138 \text{ fb}^{-1}$  data. We have the choice to extract the  $m_t$  either from the reconstructed shapes at the detector level or from the unfolded shapes at the generator level. The advantage of the latter, as proposed in Ref [11], is that once theoretical calculation is available, it could be used to extract the pole mass instead of the MC mass. For this reason, here we use the generator distribution to derive the sensitivity. To have a realistic estimation of selection efficiency and statistical loss due to the unfolding procedure, we downscale the number of events so that the statistical uncertainty of  $m_t$  derived from  $m_{\text{jet}}$  is the same as the CMS result in Ref. [11]. For the comparison between the two variables, we assume the unfolding impact is similar and the same downscale factor is applied to both distributions.

Figure 1 shows the E3C and  $m_{\text{jet}}$  distribution built from the boosted jet. All the hadrons inside the jet are used for the calculation. A peak is observed for both observables, which originated from the top quark decay, and is sensitive to the  $m_t$ , as shown by the distributions of various  $m_t$  values. For the  $m_{\text{jet}}$ , this is rather straightforward to

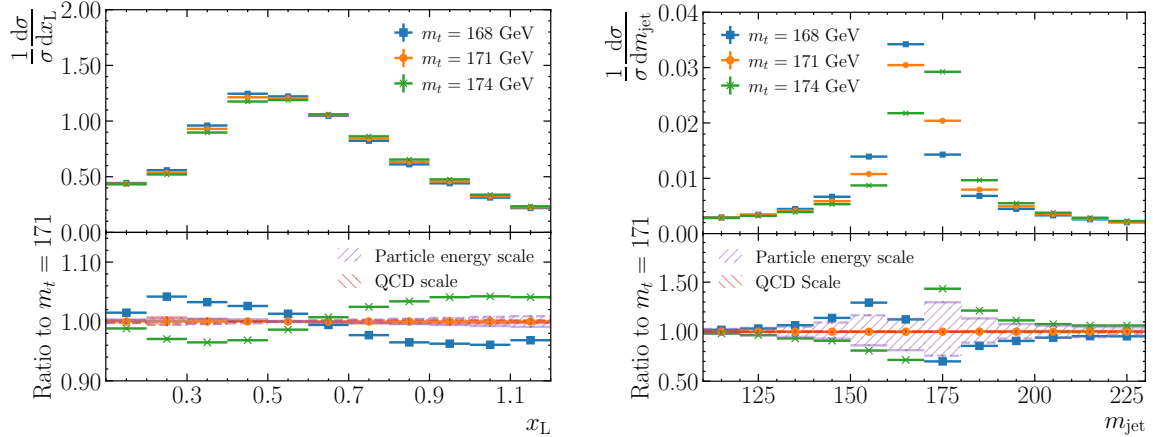


**Figure 1.** The distribution of E3C (left) and  $m_{\text{jet}}$  (right) of boosted top jets with different  $m_t$  values and their ratio to  $m_t = 171$  GeV. The leading systematic uncertainties are shown in hatched bands in the ratio panel. Here the photon, charged, and neutral particle energy scales are combined into the total particle energy scale.

understand. As for the E3C, it could be explained by  $x_L \propto m_t/p_T^{\text{top}}$  [20] in large  $p_T^{\text{top}}$  limit. Since  $p_T^{\text{top}}$  remains relatively constant as  $m_t$  changes, the peak position is directly proportional to the  $m_t$ . Compared to E3C, the nominal shape of  $m_{\text{jet}}$  is more sensitive to the  $m_t$ . The variation caused by a 3 GeV change in  $m_t$  is about 40% compared to 5% in the E3C. However, the same variation in  $m_{\text{jet}}$  could be caused by the jet  $p_T$  scale, as shown by the shaded distribution in Fig. 1. This is the reason why JES uncertainty plays an important role in such measurements [11]. On the other hand, the figure shows that E3C is much less affected by this uncertainty.

To evaluate the impact of various systematic uncertainties, we consider the sources that potentially dominate the two measurements from Ref. [11] and [22]. This includes the energy scale uncertainties of the particles within the jet, which is 1% for the charged particles, 3% for the photons and 5% for the neutral particles [22]. Each source affects the particles of a particular type and, consequently the overall jet  $p_T$ . The combined particle energy scale effect is analogous to the JES uncertainty, which changes the jet  $p_T$  by approximately 1-2% for the jets considered here. The initial-state (ISR) and final-state radiation (FSR) uncertainties are considered by varying the renormalization scale  $\mu$  in parton shower by 1/2 and 2. The QCD scale uncertainties that take into account the missing higher-order calculation in hard scattering processes are obtained from varying the renormalization and factorization scales independently by a factor of 0.5 and 2.

We calculate the  $\chi^2$  values as a function of the  $m_t$  under the impact of the above uncertainties for  $m_{\text{jet}}$  and E3C respectively. We take the shape of  $m_t = 171$  GeV as the nominal, and a deviation of  $\Delta\chi^2 = 1$  is used to extract the uncertainties. An integrated luminosity of  $36 \text{ fb}^{-1}$  is used. The estimated uncertainties from this analysis are presented in Fig. 2. The  $m_{\text{jet}}$  result is dominated by systematic uncertainties of the particle energy scales inside the jet, while the E3C based result is mainly limited by the statistical uncertainty. At the luminosity of  $36 \text{ fb}^{-1}$ , the E3C already yields a better overall sensitivity of

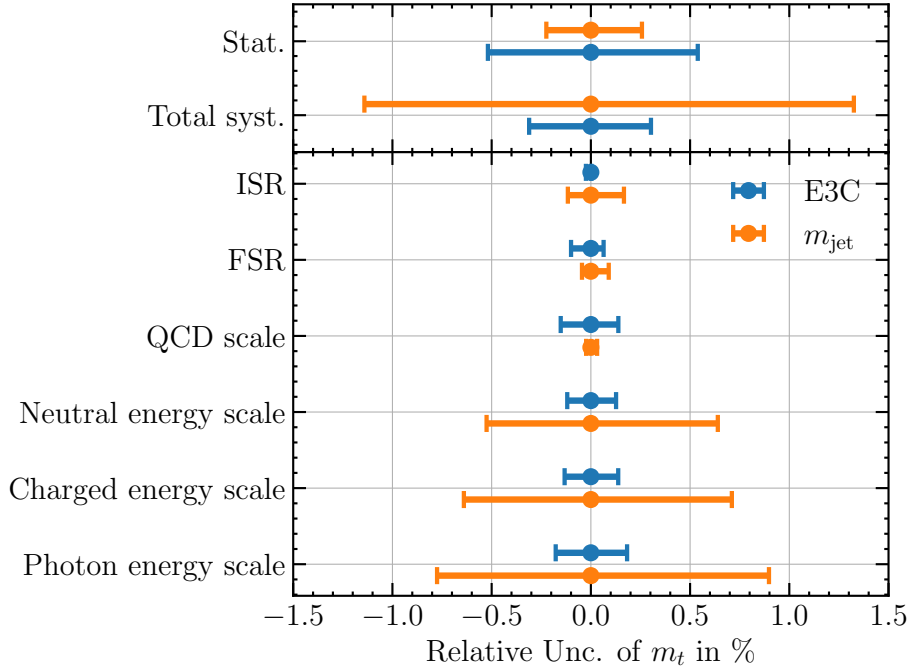


**Figure 2.** The expected uncertainties of  $m_t$  (in % of  $m_t = 171$  GeV) using E3C and  $m_{\text{jet}}$  distributions, at  $\mathcal{L} = 36 \text{ fb}^{-1}$ . The statistical uncertainties and a breakdown of the systematic uncertainties are shown.

0.6% compared to 1.2% from  $m_{\text{jet}}$ . It is expected that the E3C based result would gain more from increased statistics. At the luminosity of  $300 \text{ fb}^{-1}$ , the statistical uncertainty for E3C will decrease to 0.2%, comparable to the systematic uncertainty.

#### 4 E3C in the resolved regime

The most precise measurement of the  $m_t$  was derived in the low  $p_T^{\text{top}}$  region [10], benefiting from the large cross section. The measurement was systematic dominated and the JES was one of the major sources. The above studies in the boost regime have demonstrated that the E3C observable is much less affected by this uncertainty. The overall  $m_t$  precision would benefit more if the method could be extended to the low  $p_T^{\text{top}}$  region. Here the hadronically decayed top quark is no longer contained in a single jet, but rather becomes three well separated jets. Therefore we modify the E3C definition and treat the three jets as the constituents of the top quark, and the  $E$  in Eq. 2.1, which was the energy of the top quark jet, now becomes the sum of the energy of the three jets. Given that the four-momentum of a quark is well represented by the corresponding jet, this definition is even less affected by non-perturbative effects. For simplicity we use the kinematic information of the three quarks decayed from the top quark to demonstrate the proof of principle.

We use the semi-leptonic  $t\bar{t}$  process to check the feasibility. Events are simulated with MADGRAPH5\_aMC@NLO at LO of QCD. We focus on the events with  $p_T^{\text{top}} < 400$  GeV. The E3C is built from the three quarks that hadronically decayed from the top quark. As the

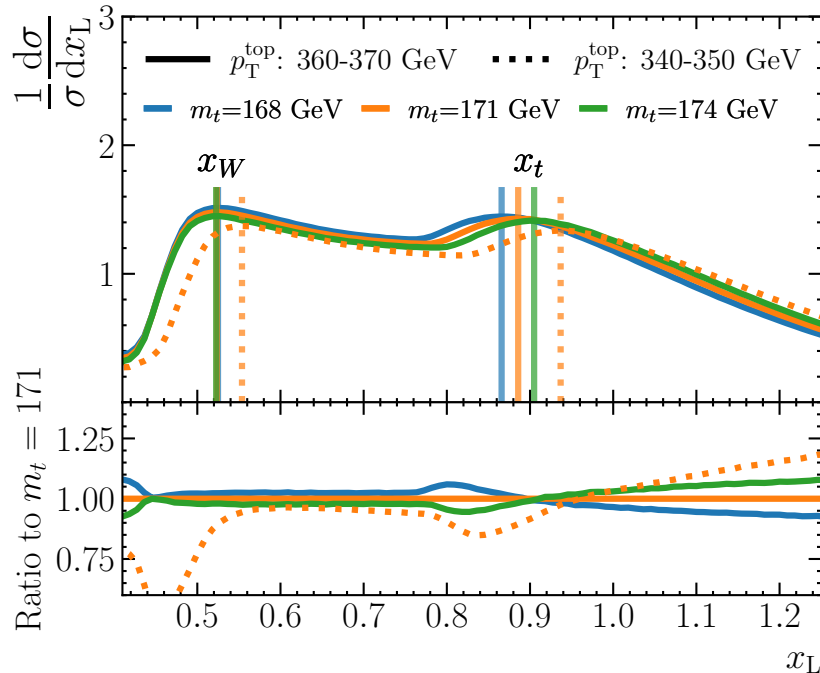


**Figure 3.** E3C distributions in the resolved regime in the range of  $360 < p_T^{\text{top}} < 370$  GeV and  $340 < p_T^{\text{top}} < 350$  GeV. The three quarks decayed from the top quark are used to build E3C. A comparison between the distributions with different  $m_t$  values is presented.

$p_T^{\text{top}}$  becomes comparable with the top quark mass, the dependence of the  $x_L$  on  $p_T^{\text{top}}$  and  $m_t$  becomes nontrivial. To differentiate the impact of the  $p_T^{\text{top}}$  and  $m_t$ , we split the events into slices of  $p_T^{\text{top}}$ .

Figure 3 shows the E3C distribution in two  $p_T^{\text{top}}$  ranges: 360–370 GeV and 340–350 GeV. In each  $p_T^{\text{top}}$  range, two distinct peaks are observed, and a structure arises from distinct decays of the W boson and top quark. We simulate events with different  $m_t$  values while keeping the  $m_W$  fixed to 80.4 GeV, as shown in Fig. 3. The right peak shifts with the  $m_t$  while the left peak stays unchanged. This feature makes the E3C a nice observable to calibrate the  $m_t$  through  $m_W$ . In earlier experimental measurements, this was achieved by constructing several observables from different inputs [10]. However, the dominant systematic uncertainties in extracting  $m_t$  and  $m_W$  may not fully overlap and are well constrained in multiple observables. While in the case of E3C, consistent inputs are used to construct a single observable, resulting in a better constraint on the uncertainties.

Similar to the approach in the boosted regime, the shape of the E3C can be used to measure  $m_t$  in the resolved regime. The overall E3C distribution depends on  $p_T^{\text{top}}$  as shown in Fig. 3, therefore a joint measurement of E3C across multiple  $p_T^{\text{top}}$  regions could improve the sensitivity. However, this also makes the measurement potentially prone to the JES: a genuine  $p_T^{\text{top}} = 345$  GeV event, corresponding to the dashed curve in Fig 3, might be reconstructed as  $p_T^{\text{top}} = 365$  GeV due to higher JES. If the distribution exhibited a single peak, similar to the often-used reconstructed  $m_t$  in experimental measurements,

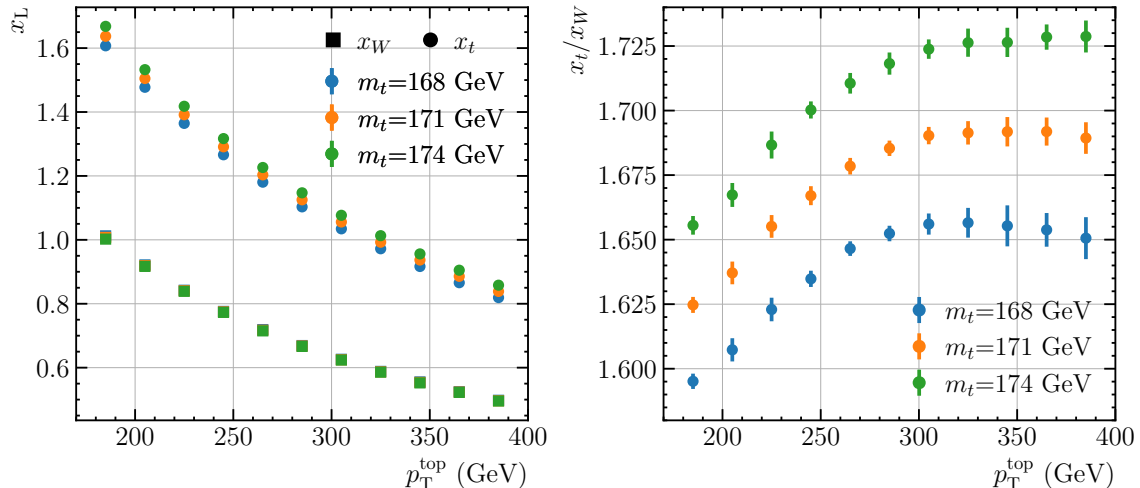


**Figure 4.** The peak position of  $x_W$  and  $x_t$  (left) and  $x_t/x_W$  (right) in the E3C distributions as a function of average  $p_T^{\text{top}}$ . The values are fitted from distributions under different  $m_t$  assumptions.

this curve could be interpreted as either a higher  $m_t$  or a higher JES, causing a large systematic uncertainty on the  $m_t$ . However, the W peak on the left helps to disentangle the two effects: both peaks move with JES, and only the top peak shifts with  $m_t$  variation, as shown in the ratio panel of Fig. 3. The two peak structure of E3C helps to reduce the impact of JES uncertainty significantly and provide a new method for experimental measurements.

The observation that both peaks in the E3C distribution shift together with  $p_T^{\text{top}}$  raises the question of whether the ratio between them is less sensitive to  $p_T^{\text{top}}$ . This could be explored to further reduce the uncertainty. To quantify that, we perform a fit to identify the  $x_L$  value corresponding to the two peaks, which we denote as  $x_W$  and  $x_t$  respectively. We use an exponentially modified Gaussian function in LMFIT package [35] to fit the E3C distribution near the peaks. The fit range of  $x_L$  is determined by requiring the  $\chi^2/n. \text{ d.f.} < 2$ . To take into account the impact of the fit range, we vary the nominal range by 10% and take the difference between the determined peaks from the fits as a systematic uncertainty. The results are shown in Fig. 4. The left figure shows the extracted  $x_t$  and  $x_W$  as a function of the average  $p_T^{\text{top}}$  in each region. Both  $x_t$  and  $x_W$  decreases with increasing  $p_T^{\text{top}}$ . Under different  $m_t$  assumptions, the  $x_W$  overlaps while the  $x_t$  shows a sensitivity to the  $m_t$  value. The right figure shows the ratio of  $x_t/x_W$  as a function of  $p_T^{\text{top}}$ . The ratio has a rather strong dependency on  $p_T^{\text{top}}$  in the relatively low  $p_T$  region, while in the range above 300 GeV, it becomes flatter. Experimental measurements could use the  $x_t/x_W$  ratio in this region to reduce the sensitivity to any uncertainties that cause migrations in the reconstructed  $p_T^{\text{top}}$ .

So far, we have focused on introducing the idea of using E3C and its feature to measure the top quark mass in the resolved regime and discussing its advantages. It is expected that further work is needed to apply it to real measurements and assess a realistic sensitivity, e.g. how to correctly pick the three quarks (jets) decayed from the top quark and how

much the wrong combinations affect the overall sensitivity. However, we expect such a background to have a rather different shape, which could be modeled and subtracted using simulations. We leave these optimizations to experimental studies.

## 5 Conclusions

In summary, we explored the potential of using E3C to determine the top quark mass in both resolved and boosted regimes. In the boosted regime, we showed that E3C provides a better mass sensitivity compared to the traditional jet mass observable in terms of systematic uncertainties, and is expected to benefit more from the increased statistics at the LHC. In the resolved regime, the presence of two distinct peaks in the E3C distribution, corresponding to the top quark and the W boson, helps to calibrate the top quark mass and constrain jet energy scale uncertainties greatly. These results demonstrate that E3C could be a promising observable for achieving high-precision measurement of the top quark mass.

## Acknowledgments

We thank Huaxing Zhu for the useful discussions. The work is supported by National Natural Science Foundation of China (NSFC) under the Grant No. 12322504 and the center for high energy physics in Peking University.

## References

- [1] S. Alekhin, A. Djouadi and S. Moch, *The top quark and Higgs boson masses and the stability of the electroweak vacuum*, *Phys. Lett. B* **716** (2012) 214 [[1207.0980](#)].
- [2] G. Degrossi, S. Di Vita, J. Elias-Miro, J.R. Espinosa, G.F. Giudice, G. Isidori et al., *Higgs mass and vacuum stability in the Standard Model at NNLO*, *JHEP* **08** (2012) 098 [[1205.6497](#)].
- [3] D. Buttazzo, G. Degrossi, P.P. Giardino, G.F. Giudice, F. Sala, A. Salvio et al., *Investigating the near-criticality of the Higgs boson*, *JHEP* **12** (2013) 089 [[1307.3536](#)].
- [4] A. Andreassen, W. Frost and M.D. Schwartz, *Scale Invariant Instantons and the Complete Lifetime of the Standard Model*, *Phys. Rev. D* **97** (2018) 056006 [[1707.08124](#)].
- [5] PARTICLE DATA GROUP collaboration, *Review of Particle Physics*, *PTEP* **2022** (2022) [083C01](#).
- [6] CMS collaboration, *Review of top quark mass measurements in CMS*, [2403.01313](#).
- [7] ATLAS collaboration, *Measurement of the top quark mass in the  $t\bar{t} \rightarrow \text{lepton}+\text{jets}$  channel from  $\sqrt{s} = 8$  TeV ATLAS data and combination with previous results*, *Eur. Phys. J. C* **79** (2019) 290 [[1810.01772](#)].
- [8] CMS collaboration, *Measurement of the top quark mass using proton-proton data at  $\sqrt{s} = 7$  and 8 TeV*, *Phys. Rev. D* **93** (2016) 072004 [[1509.04044](#)].
- [9] CMS collaboration, *Measurement of the top quark mass in the all-jets final state at  $\sqrt{s} = 13$  TeV and combination with the lepton+jets channel*, *Eur. Phys. J. C* **79** (2019) 313 [[1812.10534](#)].



- [10] CMS collaboration, *Measurement of the top quark mass using a profile likelihood approach with the lepton + jets final states in proton–proton collisions at  $\sqrt{s} = 13$  TeV*, *Eur. Phys. J. C* **83** (2023) 963 [2302.01967].
- [11] CMS collaboration, *Measurement of the Jet Mass Distribution and Top Quark Mass in Hadronic Decays of Boosted Top Quarks in  $pp$  Collisions at  $\sqrt{s} = 13$  TeV*, *Phys. Rev. Lett.* **124** (2020) 202001 [1911.03800].
- [12] CMS collaboration, *Measurement of the top quark mass using events with a single reconstructed top quark in  $pp$  collisions at  $\sqrt{s} = 13$  TeV*, *JHEP* **12** (2021) 161 [2108.10407].
- [13] CMS collaboration, *Measurement of the top quark pole mass using  $t\bar{t}$ +jet events in the dilepton final state in proton–proton collisions at  $\sqrt{s} = 13$  TeV*, *JHEP* **07** (2023) 077 [2207.02270].
- [14] ATLAS collaboration, *Top-quark mass measurement in the all-hadronic  $t\bar{t}$  decay channel at  $\sqrt{s} = 8$  TeV with the ATLAS detector*, *JHEP* **09** (2017) 118 [1702.07546].
- [15] CMS collaboration, *Measurement of the top quark mass using charged particles in  $pp$  collisions at  $\sqrt{s} = 8$  TeV*, *Phys. Rev. D* **93** (2016) 092006 [1603.06536].
- [16] CMS collaboration, *Measurement of the mass of the top quark in decays with a  $J/\psi$  meson in  $pp$  collisions at 8 TeV*, *JHEP* **12** (2016) 123 [1608.03560].
- [17] ATLAS collaboration, *Measurement of the  $t\bar{t}$  production cross-section using  $e\mu$  events with  $b$ -tagged jets in  $pp$  collisions at  $\sqrt{s} = 7$  and 8 TeV with the ATLAS detector*, *Eur. Phys. J. C* **74** (2014) 3109 [1406.5375].
- [18] ATLAS collaboration, *Measurement of the top-quark mass using a leptonic invariant mass in  $pp$  collisions at  $\sqrt{s} = 13$  TeV with the ATLAS detector*, *JHEP* **06** (2023) 019 [2209.00583].
- [19] CMS collaboration, *Measurement of the differential  $t\bar{t}$  production cross section as a function of the jet mass and extraction of the top quark mass in hadronic decays of boosted top quarks*, *Eur. Phys. J. C* **83** (2023) 560 [2211.01456].
- [20] J. Holguin, I. Moul, A. Pathak and M. Procura, *New paradigm for precision top physics: Weighing the top with energy correlators*, *Phys. Rev. D* **107** (2023) 114002 [2201.08393].
- [21] J. Holguin, I. Moul, A. Pathak, M. Procura, R. Schöffbeck and D. Schwarz, *Using the  $W$  as a Standard Candle to Reach the Top: Calibrating Energy Correlator Based Top Mass Measurements*, 2311.02157.
- [22] CMS collaboration, *Measurement of energy correlators inside jets and determination of the strong coupling  $\alpha_S(m_Z)$* , 2402.13864.
- [23] C.L. Basham, L.S. Brown, S.D. Ellis and S.T. Love, *Energy Correlations in electron - Positron Annihilation: Testing QCD*, *Phys. Rev. Lett.* **41** (1978) 1585.
- [24] L.J. Dixon, I. Moul and H.X. Zhu, *Collinear limit of the energy-energy correlator*, *Phys. Rev. D* **100** (2019) 014009 [1905.01310].
- [25] K. Lee, B. Meçaj and I. Moul, *Conformal Colliders Meet the LHC*, 2205.03414.
- [26] H. Chen, I. Moul, X. Zhang and H.X. Zhu, *Rethinking jets with energy correlators: Tracks, resummation, and analytic continuation*, *Phys. Rev. D* **102** (2020) 054012 [2004.11381].
- [27] W. Chen, J. Gao, Y. Li, Z. Xu, X. Zhang and H.X. Zhu, *NNLL resummation for projected three-point energy correlator*, *JHEP* **05** (2024) 043 [2307.07510].

- [28] CMS, ATLAS collaboration, *Combination of measurements of the top quark mass from data collected by the ATLAS and CMS experiments at  $\sqrt{s} = 7$  and 8 TeV*, [2402.08713](#).
- [29] J. Alwall, R. Frederix, S. Frixione, V. Hirschi, F. Maltoni, O. Mattelaer et al., *The automated computation of tree-level and next-to-leading order differential cross sections, and their matching to parton shower simulations*, *JHEP* **07** (2014) 079 [[1405.0301](#)].
- [30] R. Frederix, S. Frixione, V. Hirschi, D. Pagani, H.S. Shao and M. Zaro, *The automation of next-to-leading order electroweak calculations*, *JHEP* **07** (2018) 185 [[1804.10017](#)].
- [31] C. Bierlich et al., *A comprehensive guide to the physics and usage of PYTHIA 8.3*, *SciPost Phys. Codeb.* **2022** (2022) 8 [[2203.11601](#)].
- [32] M. Cacciari, G.P. Salam and G. Soyez, *The anti- $k_t$  jet clustering algorithm*, *JHEP* **04** (2008) 063 [[0802.1189](#)].
- [33] M. Cacciari and G.P. Salam, *Dispelling the  $N^3$  myth for the  $k_t$  jet-finder*, *Phys. Lett. B* **641** (2006) 57 [[hep-ph/0512210](#)].
- [34] M. Cacciari, G.P. Salam and G. Soyez, *FastJet User Manual*, *Eur. Phys. J. C* **72** (2012) 1896 [[1111.6097](#)].
- [35] M. Newville, T. Stensitzki, D.B. Allen and A. Ingargiola, *LMFIT: Non-Linear Least-Square Minimization and Curve-Fitting for Python*, Oct., 2015. [10.5281/zenodo.11813](#).